

A PHENOMENOLOGICAL ANALYSIS OF THE WEINBERG SUM RULES AND OF THE $\pi^+ - \pi^0$ MASS DIFFERENCE

R.D. PECCEI and J SOLÀ*

DESY, Hamburg, Fed. Rep. Germany

Received 8 July 1986

We use recent data on τ -lepton hadronic decays to extract the q^2 dependent vector and axial-vector spectral functions. Even though our results are necessarily restricted kinematically, we make use of these experimentally determined spectral functions to check to what extent the Weinberg sum rules are satisfied and to compute the pion electromagnetic mass difference. Although the results we obtain are satisfactory, the agreement with theoretical expectations appears to be somewhat fortuitous. A much more relevant and reliable theoretical comparison is provided by a Laplace transform version of the sum rules, which is more convergent and for which the QCD corrections are under better control.

A very important early step in the theory of the weak interactions was the realization that the currents which enter in weak decays are also the (approximate) symmetry currents of the strong interactions [1]. This deep interconnection is now simply understood in the standard model of the strong and electroweak interactions in terms of invariances related to the quark degrees of freedom. QCD, in the limit in which one neglects the mass for the u and d quarks, has a global $SU(2)_R \times SU(2)_L$ symmetry in which the quark doublets are transformed as:

$$\begin{aligned} q_L &\equiv \begin{pmatrix} u \\ d \end{pmatrix}_L \rightarrow e^{i\alpha_L \tau_a / 2} \begin{pmatrix} u \\ d \end{pmatrix}_L, \\ q_R &\equiv \begin{pmatrix} u \\ d \end{pmatrix}_R \rightarrow e^{i\alpha_R \tau_a / 2} \begin{pmatrix} u \\ d \end{pmatrix}_R. \end{aligned} \quad (1)$$

The symmetry currents for these transformations are conventionally written in terms of the vector and axial currents:

$$\begin{aligned} V_a^\mu &= \bar{q} \gamma^\mu \frac{\tau_a}{2} q, \\ A_a^\mu &= \bar{q} \gamma^\mu \gamma_5 \frac{\tau_a}{2} q. \end{aligned} \quad (2)$$

* On leave of absence from Department de Física de la Universitat Autònoma de Barcelona, Spain

Because the left-handed u and d quarks transform as a doublet under the electro-weak SU(2) group, it is clear that, as far as the u and d quarks go, the weak SU(2) current is simply related to V_a^μ and A_a^μ . One has

$$J_a^\mu = \bar{q}_L \gamma^\mu \frac{\tau_a}{2} q_L = \frac{1}{2} (V_a^\mu - A_a^\mu). \quad (3)$$

This interrelationship has been used in the past to predict certain features of weak decays (for example weak magnetism [2]) from properties of the strong currents. Here we would like to do the reverse and use weak decay results to infer structural properties related to the strong symmetry currents. More specifically, we shall analyze recent data on the semileptonic decays of the τ lepton to extract information on the q^2 dependence of the spectral functions connected with the vector and axial currents of eq. (2). Having these results in hand, we shall then examine how well do certain sum rules, based on the global symmetries of QCD, work and attempt to compute the $\pi^+ - \pi^0$ electromagnetic mass difference.

It is convenient to write down a spectral decomposition for the two-point correlation functions associated with the currents V_a^μ and A_a^μ . One has:

$$\begin{aligned} & i \langle 0 | T(V_a^\mu(x) V_b^\nu(0)) | 0 \rangle \\ &= \delta_{ab} \int \frac{d^4 p}{(2\pi)^4} e^{ipx} \int \frac{dM^2}{p^2 + M^2 - i\epsilon} \left\{ \rho_V(M^2) (M^2 \eta^{\mu\nu} + p^\mu p^\nu) \right. \\ & \qquad \qquad \qquad \left. + \rho_V^0(M^2) p^\mu p^\nu \right\} + \text{S.T.}, \quad (4a) \end{aligned}$$

$$\begin{aligned} & i \langle 0 | T(A_a^\mu(x) A_b^\nu(0)) | 0 \rangle \\ &= \delta_{ab} \int \frac{d^4 p}{(2\pi)^4} e^{ipx} \int \frac{dM^2}{p^2 + M^2 - i\epsilon} \left\{ \rho_A(M^2) (M^2 \eta^{\mu\nu} + p^\mu p^\nu) \right. \\ & \qquad \qquad \qquad \left. + \rho_A^0(M^2) p^\mu p^\nu \right\} + \text{S.T.}. \quad (4b) \end{aligned}$$

In the above S.T. stands for possible Schwinger terms [3] which, however, will play no role in our considerations. In what follows, we shall be mostly interested in the chiral limit, where $m_u = m_d = 0$. In this case the longitudinal vector spectral function ρ_V^0 vanishes, while the corresponding axial spectral function has only a contribution from the Goldstone pions:

$$\begin{aligned} \rho_V^0(M^2) &= 0, \\ \rho_A^0(M^2) &= f_\pi^2 \delta(M^2) \quad (\text{chiral limit}). \quad (5) \end{aligned}$$

Here $f_\pi \approx 93.3$ MeV, is the pion decay constant. In principle the vector and axial spectral functions are calculable in QCD, but in practice we are still very far away from being able to do that in the low-energy region. However, because of the connection of V_a^μ and A_a^μ with the weak current (eq. (3)) it is possible to infer experimentally some information about ρ_V and ρ_A by studying the semileptonic decays of the τ -lepton. Of course, in these decays the accessible M^2 range is restricted to be below m_τ^2 . However, as we shall see, one already obtains important information, even within this narrow kinematical range.

Almost twenty years ago, Weinberg [4] derived two sum rules for ρ_V and ρ_A , using some general arguments related to the expected asymptotic behaviour of strong interaction processes. Weinberg's sum rules read

$$\int dM^2 (\rho_V(M^2) - \rho_A(M^2)) = f_\pi^2, \quad (6)$$

$$\int dM^2 M^2 (\rho_V(M^2) - \rho_A(M^2)) = 0. \quad (7)$$

One can show that these sum rules, obtained before the development of QCD as a theory of the strong interactions, are actually valid in QCD in the chiral limit [5]. However, when quark masses are included only the first Weinberg sum rule, when appropriately reinterpreted, remains valid. The second sum rule breaks down since, in perturbation theory, the spectral function difference receives contributions of order m_q^2/M^2 , which lead to a quadratic divergence. One can, nevertheless, construct appropriately weighted combinations of the transverse and longitudinal spectral functions which lead to convergent Weinberg sum rules of the second kind [5]. In QCD, the first Weinberg sum rule is replaced by:

$$\int dM^2 [(\rho_V(M^2) - \rho_A(M^2)) + (\rho_V^{(0)}(M^2) - \rho_A^{(0)}(M^2))] = 0. \quad (8)$$

Recalling eq. (5), one sees that in the chiral limit the second term above precisely reproduces the f_π^2 factor of eq. (6). Note also that although in QCD the transverse and longitudinal spectral functions contain terms of order m_q^2/M^2 these terms cancel each other in eq. (8) [5].

Rather than giving a modified second Weinberg sum rule in QCD, it is more useful to consider, following the original suggestion of Shifman, Vainshtein and Zakharov [6], a Laplace transformed version of these sum rules. For these Laplace transform sum rules one introduces an extra scale κ^2 and, in effect, one is then dealing with an infinite set of relations, one for each value of κ^2 . Because the Laplace transform sum rules contain a weight e^{-M^2/κ^2} their convergence in QCD is controlled by a series of operator expectation values of increasing dimensionality each weighted by an appropriate κ^2 factor.

Corresponding to the first Weinberg sum rule, one has [5, 7, 8]:

$$\begin{aligned} & \int_0^\infty dM^2 e^{-M^2/\kappa^2} \{ (\rho_V(M^2) - \rho_A(M^2)) + (\rho_V^{(0)}(M^2) - \rho_A^{(0)}(M^2)) \} \\ &= \frac{\alpha_s(\kappa^2)}{2\pi} \left\{ -\frac{\bar{m}_u(\kappa^2)\bar{m}_d(\kappa^2)}{\pi^2} \right. \\ & \quad \left. + \frac{8}{3} \frac{(m_u + m_d)\langle 0|\bar{u}u|0\rangle}{\kappa^2} - \frac{32}{9}\pi \frac{(\langle 0|\bar{q}q|0\rangle)^2}{\kappa^4} + \dots \right\}, \quad (9) \end{aligned}$$

where $\alpha_s(\kappa^2)$ and $\bar{m}(\kappa^2)$ are the QCD running coupling and mass, respectively. Since the r.h.s. of eq. (9) vanishes as $\kappa^2 \rightarrow \infty$, one recovers immediately in this limit the first Weinberg sum rule, eq. (8). More importantly, already for moderate values of κ^2 , of $O(\text{GeV}^2)$, one sees that the corrections on the r.h.s. of eq. (9) are *small* compared to f_π^2 . Hence, using these Laplace transform sum rules, one may well be able to test the expectations of QCD, using values of ρ_V and ρ_A obtained for moderate values of M^2 .

The Laplace transform version of the second Weinberg sum rule (7) reads [5, 7, 8]:

$$\begin{aligned} & \int dM^2 M^2 e^{-M^2/\kappa^2} (\rho_V(M^2) - \rho_A(M^2)) \\ &= \frac{3\kappa^2}{4\pi^2} \bar{m}_u(\kappa^2)\bar{m}_d(\kappa^2) - (m_u + m_d)\langle 0|\bar{u}u|0\rangle + O(1/\kappa^2). \quad (10) \end{aligned}$$

It is now no longer possible to take the limit of $\kappa^2 \rightarrow \infty$, and therefore recover the second Weinberg sum rule, except in the chiral limit. Note that the badly divergent term is of second order in the quark masses. To first order in the quark masses the second Weinberg sum rule eq. (7) receives a finite contribution

$$\text{l.h.s} = -(m_u + m_d)\langle 0|\bar{u}u|0\rangle = f_\pi^2 m_\pi^2, \quad (11)$$

where we have used the usual current algebra expression for the pion mass [9]. The $\pi^+ - \pi^0$ electromagnetic mass difference can be calculated in principle using the vector and axial-vector spectral functions. Using current algebra techniques Das, Guralnik, Mathur, Low and Young [10] derived the classic formula

$$m_{\pi^+}^2 - m_{\pi^0}^2 = \frac{12\pi\alpha}{f_\pi^2 i} \int \frac{d^4q}{(2\pi)^4} \frac{1}{q^2} \int_0^\infty dM^2 M^2 \frac{[\rho_V(M^2) - \rho_A(M^2)]}{q^2 + M^2 - i\epsilon}. \quad (12)$$

If the second Weinberg sum rule holds – as is the case in the chiral limit – eq. (12)

yields a finite result. This result is expected in QCD from an analysis of the short-distance expansion of the product of two electromagnetic currents [11]. However, if one retains terms of first order in the quark masses, one can show that the pion electromagnetic mass difference will then exhibit a logarithmic divergence, proportional to $(m_u + m_d)\langle 0|\bar{u}u|0\rangle$ [11]. This result follows directly also from eq. (12), using eq. (11) as the l.h.s. of the second Weinberg sum rule. The presence of this divergence should not be troubling since it can be absorbed by a redefinition of the quark mass terms. Indeed, since in QCD one is near the chiral limit, it is sensible to attempt to evaluate (12) using whatever information is available on the spectral functions. In fact, this is precisely what Das et al. [10] did. They assumed that ρ_V and ρ_A are saturated by the ρ and A_1 mesons respectively and, using the Weinberg sum rules and the KSFR relation [12], obtained $m_{\pi^+} - m_{\pi^0} = 5$ MeV, in amazing agreement with the experimental value of 4.6 MeV. We will repeat this analysis using the spectral functions that we will determine from τ decay, to which we now turn.

The amplitude for the semileptonic decay of the τ lepton into non-strange hadrons ($S = 0$) in the 4-Fermi approximation, reads:

$$\begin{aligned} A(\tau^\pm \rightarrow \nu_\tau + \text{hadrons}(S=0)) \\ = \sqrt{2} G_F \cos \theta_C \bar{u}(p_\nu) \gamma_\mu (1 - \gamma_5) u(p_\tau) \\ \times \langle \text{hadrons}(S=0) | J_{1+i_2}^\mu | 0 \rangle. \end{aligned} \quad (13)$$

If the $S = 0$ hadrons are an even number of pions then only $V_{1+i_2}^\mu$ contributes in eq. (13), while for an odd number of pions only $A_{1+i_2}^\mu$ contributes. Thus the differential transition probabilities per invariant mass squared, for the process $\tau \rightarrow \nu_\tau n\pi$ will be a measure of ρ_V and ρ_A , respectively, depending on whether n is even or odd. Using eq. (13) and the definition of the spectral functions in eqs. (4), neglecting the longitudinal pieces, one arrives at the general formula [13]

$$\sum_n \frac{d\Gamma(\tau \rightarrow \nu_\tau + n\pi)}{dM^2} = \frac{G_F^2 \cos^2 \theta_C}{32\pi^2 m_\tau^3} (m_\tau^2 + 2M^2)(m_\tau^2 - M^2)^2 \left\{ \begin{array}{l} v(M^2) \\ a(M^2) \end{array} \right\}, \quad (14)$$

where the upper line applies for n even and the lower line for n odd ($n > 1$). Here v and a are simply related to the spectral functions ρ_V and ρ_A by

$$\begin{aligned} v(M^2) &= 4\pi\rho_V(M^2), \\ a(M^2) &= 4\pi\rho_A(M^2). \end{aligned} \quad (15)$$

Apart from the single pion decay $\tau \rightarrow \nu_\tau \pi$, the most important decay channels for

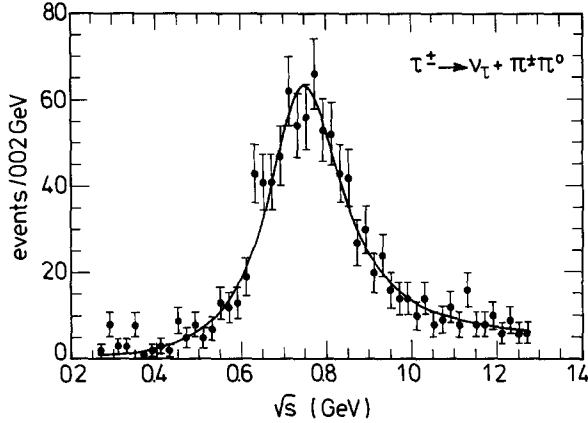


Fig. 1. Fit of the invariant mass $\sqrt{s} = M_{2\pi}$ distribution for the decay $\tau^\pm \rightarrow \nu_\tau + \pi^\pm \pi^0$

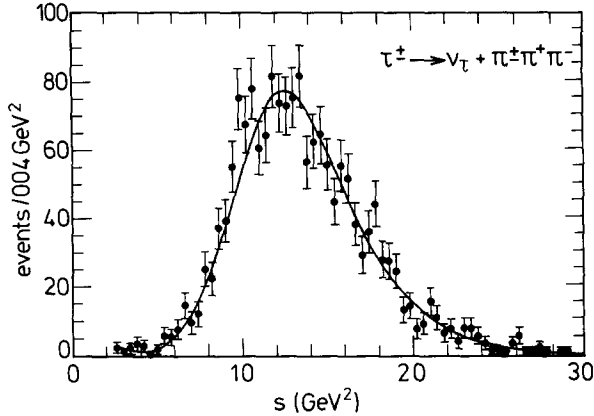


Fig. 2. Fit of the invariant mass squared $s = M_{3\pi}^2$ distribution for the decay $\tau^\pm \rightarrow \nu_\tau + \pi^\pm \pi^+ \pi^-$

the τ involve two, three and four pions, for which we have detailed experimental information. There exist no precise data on higher multiplicity final states like $\tau \rightarrow \nu_\tau 5\pi$ or $\tau \rightarrow \nu_\tau 6\pi$, but these contributions are thought to be negligible [14, 15]. As far as the dominant decays go, we will base our analysis mostly on recent data obtained by the Argus collaboration at DORIS [16, 17]. The relevant distributions for the one-prong channel $\tau^\pm \rightarrow \nu_\tau \pi^\pm \pi^0$ and for the three prong channels $\tau^\pm \rightarrow \nu_\tau \pi^\pm \pi^+ \pi^-$ and $\tau^\pm \rightarrow \nu_\tau \pi^\pm \pi^+ \pi^- \pi^0$ are shown, respectively, in figs. 1, 2 and 3. The one-prong distribution of fig. 1 is not acceptance corrected (and it is plotted for convenience against \sqrt{s} not s). However, this distribution is quite comparable to the data published by the Mark II collaboration [18], and so we believe that these corrections are not of major importance, as this mode is essentially dominated by

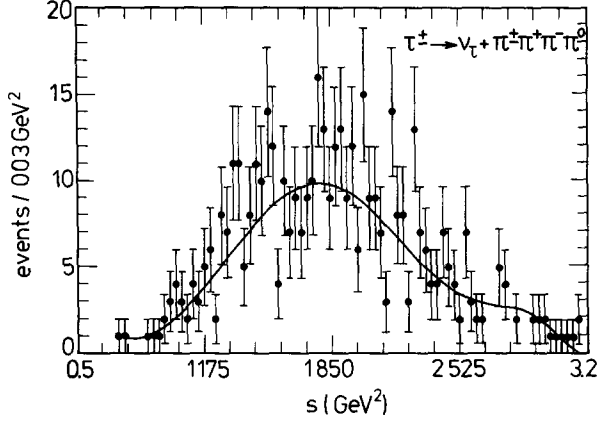


Fig. 3 Fit of the invariant mass squared $s = M_{4\pi}^2$ distribution for the decay $\tau^\pm \rightarrow \nu_\tau + \pi^\pm \pi^+ \pi^- \pi^0$.

the ρ^\pm . Indeed we have checked that our fit of the data in fig. 1 is in good agreement with the ρ -dominated spectral function obtained from a study of the reaction $e^+e^- \rightarrow \pi^+\pi^-$ [19]. There is, as yet, no experimental information on the multipion one-prong channels $\tau^\pm \rightarrow \nu_\tau \pi^\pm \pi^0 \pi^0$ and $\tau^\pm \rightarrow \nu_\tau \pi^\pm \pi^0 \pi^0 \pi^0$. However, to the extent that the data for the channel $\tau^\pm \rightarrow \nu_\tau \pi^\pm \pi^+ \pi^-$ shows a very strong A_1 resonance dominance [17,20], one may estimate the $\tau^\pm \rightarrow \nu_\tau \pi^\pm \pi^0 \pi^0$ contribution simply by isospin symmetry, in which case one has

$$\begin{aligned} B(\tau^\pm \rightarrow \nu_\tau \pi^\pm \pi^0 \pi^0) &= B(\tau^\pm \rightarrow \nu_\tau \pi^\pm \pi^+ \pi^-) \\ &= (5.6 \pm 0.7)\%, \end{aligned} \quad (16)$$

where the numerical result is that obtained by Argus [17]. Gilman and Rhie [14] using e^+e^- data and CVC have estimated that the branching ratio for the channel $\tau^\pm \rightarrow \nu_\tau \pi^\pm 3\pi^0$ is about 5 times smaller than that for the three-prong decay $\tau^\pm \rightarrow \nu_\tau \pi^\pm \pi^+ \pi^- \pi^0$. Since the branching ratio for this latter mode is not very large [16]

$$B(\tau^\pm \rightarrow \nu_\tau \pi^\pm \pi^+ \pi^- \pi^0) = (4.5 \pm 0.4 \pm 1.5)\% \quad (17)$$

and the error is considerable, we shall totally ignore the channel $\tau \rightarrow \nu_\tau \pi^\pm 3\pi^0$ in our analysis. Hence our results will be based on the distributions shown in figs. 1–3, augmented by the isospin relation [16].

The curves shown in figs. 1–3 are our best χ^2 fits for these distributions, using the numerical program MINUIT. For figs. 1 and 2 we have used a Breit-Wigner function convoluted with a high order background polynomial. In fig. 3, where there is no apparent sharp resonance behaviour we just used a high order polynomial. On

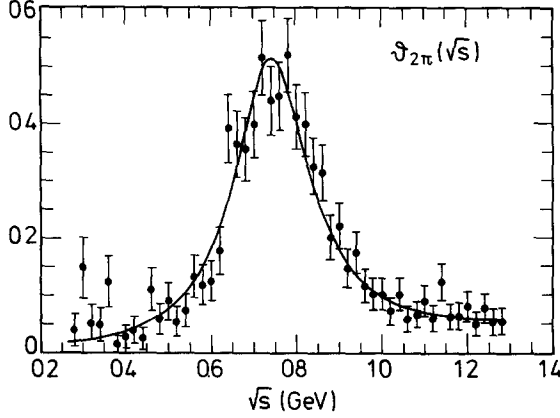


Fig. 4. Fit of the spectral function $v_{\pi^{\pm}\pi^0}$ for the decay of fig. 1 as a function of the invariant mass $\sqrt{s} = M_{2\pi}$.

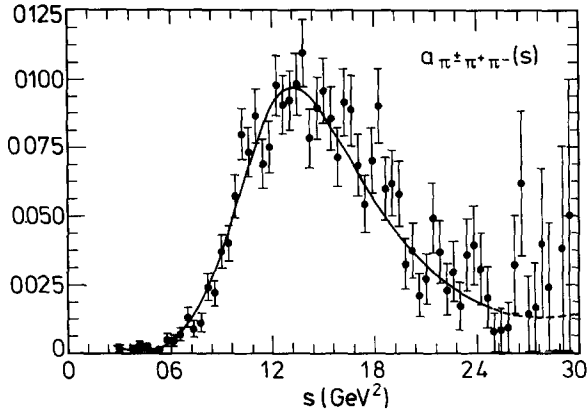


Fig. 5. Fit of the spectral function $a_{\pi^{\pm}\pi^+\pi^-}$ for the decay of fig. 2 as a function of the invariant mass squared $s = M_{3\pi}^2$. The dashed line, beginning at $s \approx 24 \text{ GeV}^2$, denotes the region where the error bars start to be too big for the fit to be trustworthy.

the basis of these numerical results, we have extracted the relevant spectral functions $v_{2\pi}$, $a_{\pi^{\pm}\pi^+\pi^-}$ and $v_{\pi^{\pm}\pi^+\pi^-\pi^0}$ making use of eq. (14). These are displayed in figs. 4–6 along with the data with the corresponding error bars. Note that as we approach the kinematical limit $s = m_{\pi}^2$, it becomes very difficult to extract a reliable value for the spectral functions. This is especially so for the 3π and particularly so for the 4π contribution. Thus we have indicated in figs. 5 and 6 by a dashed line the region beyond which we do not trust our fit (which is $s \geq 2 \text{ GeV}^2$ for the 4π case). We have collected our results for the spectral functions $v_{2\pi}$, $a_{3\pi} = 2a_{\pi^{\pm}\pi^+\pi^-}$ and

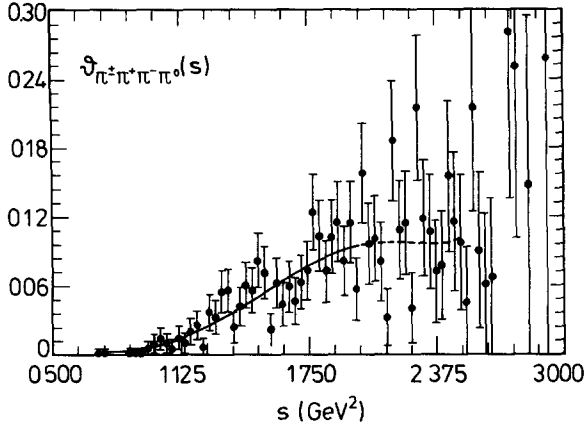


Fig. 6. Fit of the spectral function $v_{\pi^+\pi^-\pi^+\pi^0}$ for the decay in fig. 3 as a function of the invariant mass squared $s = M_{4\pi}^2$. The dashed line, beginning at about $s = 2$ GeV², denotes the region where the error bars start to be too big for the fit to be trustworthy.

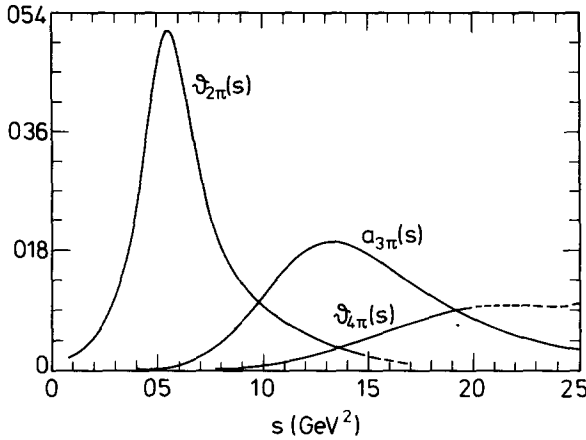


Fig. 7. The hadronic vector ($v = v_{2\pi} + v_{4\pi}$) and axial vector ($a = a_{3\pi}$) spectral functions in the low-energy region as a function of s . In this figure $a_{3\pi}$ stands for twice $a_{\pi^+\pi^-\pi^+\pi^0}$ of fig. 5 and the dashed line for $v_{4\pi}$ has the same meaning as in fig. 6.

$v_{4\pi} \approx v_{\pi^+\pi^-\pi^+\pi^0}$ in fig. 7 and it is these distributions which we shall use in our subsequent analysis.

Given that our spectral functions are only determined for $M^2 < m_\pi^2$ (In fact reliably only for $M^2 \leq 2$ GeV² and approximately reliably for $M^2 \leq 2.5$ GeV², as fig. 7 shows) it is clearly not terribly meaningful to try to test the Weinberg sum rules, where one must integrate over an infinite range! However, it is at least interesting to see how well one does when one integrates the relevant spectral

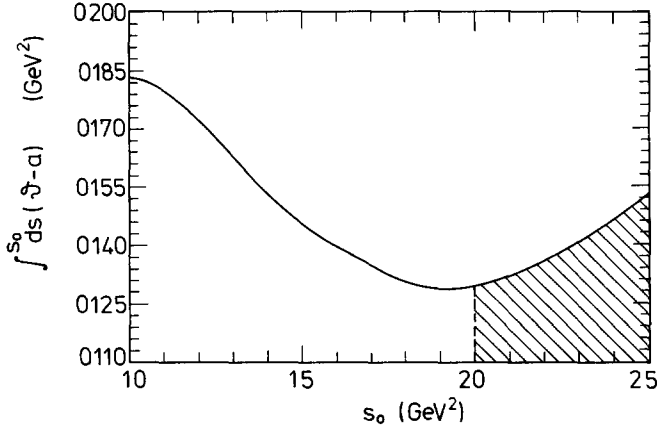


Fig. 8 The behaviour of the 1st Weinberg sum rule as a function of the upper limit of integration s_0 . The dashed area uses $v_{4\pi}$ in the questionable region of fig. 6.

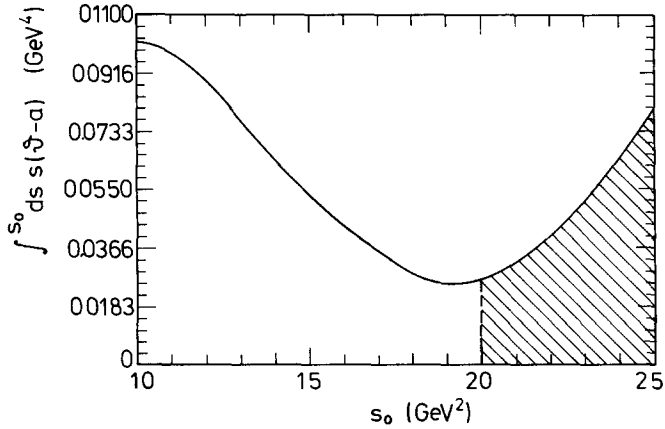


Fig. 9. The behavior of the 2nd Weinberg sum rule as a function of s_0 . The dashed area has the same meaning as that of fig. 8

function difference up to a maximum limit s_0 . We show respectively in figs. 8, 9 and 10 plots of the integrals

$$I_1(s_0) = \int_0^{s_0} ds (v(s) - a(s)), \quad (18a)$$

$$I_2(s_0) = \int_0^{s_0} ds s (v(s) - a(s)), \quad (18b)$$

$$\Delta(\pi^+ - \pi^0) = \frac{3\alpha}{32\pi^2 m_\pi f_\pi^2} \int_0^{s_0} ds s (a(s) - v(s)) \ln s. \quad (18c)$$

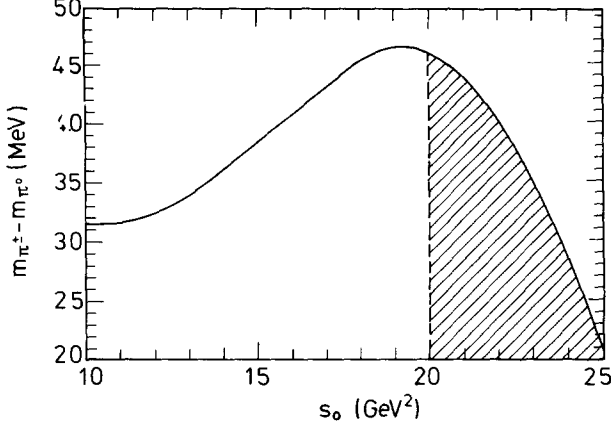


Fig. 10. The electromagnetic pion mass difference, as computed from eq. (18c) using the spectral functions of fig 7. The dashed area has the same meaning as those of figs 8 and 9.

These integrals, in the limit as $s_0 \rightarrow \infty$, reduce to the two Weinberg sum rules and an expression for the mass difference $m_{\pi^+} - m_{\pi^0}$, valid in the chiral limit where the 2nd Weinberg sum rule holds. Note that if we saturate (18c) with the ρ and A_1 contributions, and make use of the KSFR relation [12], we recover the famous formula of Das et al. [10] for $m_{\pi^+} - m_{\pi^0}$:

$$m_{\pi^+} - m_{\pi^0} = \frac{3\alpha m_\rho^2 \ln 2}{4\pi m_\pi}. \quad (19)$$

The crosshatched area in figs. 8–10 represents the region in which our determination of the spectral function is less certain. Remarkably, and surely accidentally, if we were to stop our integration range at $s_0 = 2 \text{ GeV}^2$ all three quantities in eq. (18) approach the closest to the predicted asymptotic values: $4\pi f_\pi^2 \approx 0.11 \text{ GeV}^2$, 0, and 4.6 MeV, respectively. What is perhaps not accidental, however, is that all three expressions in (18) approach closest to the predicted asymptotic value (in the chiral limit) at the *same* s_0 value. This suggests that the Weinberg sum rules and the pion electromagnetic mass difference converge in a “piecewise” fashion. That is, for higher values of M^2 other channels for ρ_V and ρ_A become important, but their contributions cancel each other out. It is for this reason that the resonance saturation formula (19) works so well. However, note that using the exact form of $v_{2\pi}$ and $a_{3\pi}$, extracted from the τ lepton semileptonic decay results, the contribution of $v_{4\pi}$ is rather important for the $\pi^+ - \pi^0$ difference. Neglecting this term, for example, at $s_0 = 2 \text{ GeV}^2$ one would obtain $\Delta(\pi^+ - \pi^0) \approx 7 \text{ MeV}$ rather than about 4.6 MeV.

In view of the uncertainties inherent in having to cut off the integration range at a given s_0 for the Weinberg sum rules, the advantage of the Laplace transform sum

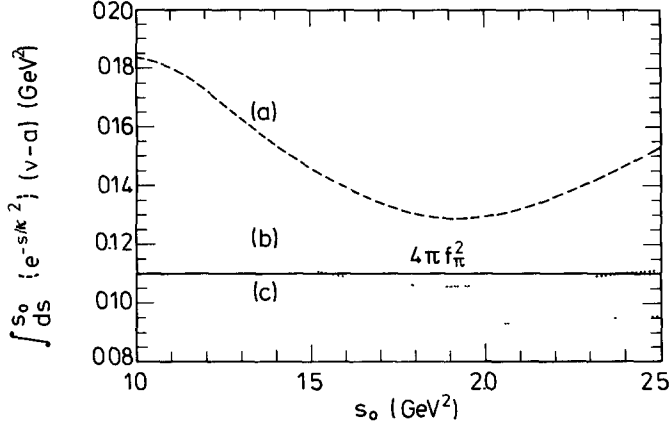


Fig. 11 A comparison between the dependence on s_0 of the normal 1st Weinberg sum rule (curve (a)) and the corresponding Laplace transform sum rule for $\kappa^2 = 1.5 \text{ GeV}^2$ (curve (b)) and $\kappa^2 = 1 \text{ GeV}^2$ (curve (c)). The straight line at $4\pi f_\pi^2 = 0.11$ is the theoretical chiral limit prediction.

rules of eqs. (9) and (10) is obvious. By choosing κ^2 sufficiently *small*, the contribution of the spectral functions much beyond this κ^2 are exponentially suppressed. On the other hand, if κ^2 is *large* enough, then the perturbative contributions on the r.h.s. of the sum rules are also small. For our purposes, values of $\kappa^2 \sim (1.0-1.5) \text{ GeV}^2$ seem optimal, for then the perturbative corrections are small and we can very well approximate ρ_V and ρ_A by the contributions deduced from our τ -decay analysis.

We present in figs. 11 and 12 the contributions of the vector and axial-vector spectral functions to the, Laplace transform, integrals

$$J_1(s_0) = \int_0^{s_0} ds e^{-s/\kappa^2} (v(s) - a(s)), \quad (20a)$$

$$J_2(s_0) = \int_0^{s_0} ds s e^{-s/\kappa^2} (v(s) - a(s)), \quad (20b)$$

for various values of κ^2 as a function of s_0 . In particular, when $\kappa^2 = \infty$ then $J_i(s_0) = I_i(s_0)$ and one reduces to the truncated Weinberg sum rules already studied. Two points are clear from these figures:

(i) The results obtained for moderate κ^2 ($\kappa^2 \sim 1-1.5 \text{ GeV}^2$) are essentially independent on whether we cut off the integral at $s_0 = 2 \text{ GeV}^2$ or $s_0 = 2.5 \text{ GeV}^2$. Hence, as remarked above, these Laplace transform sum rules are very suitable for the case one knows the spectral functions only in a limited kinematical range.

(ii) The Laplace transform integral related to the 1st Weinberg sum rule appears to be in good agreement with the asymptotic QCD prediction (i.e. essentially

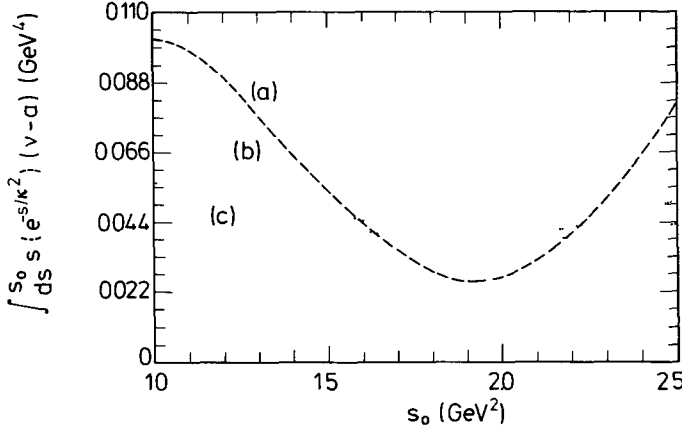


Fig. 12. As in fig 11, but now for the 2nd Weinberg sum rule and its Laplace transform version. Here the theoretical chiral limit prediction is the straight line at zero.

$4\pi f_\pi^2 = 0.11 \text{ GeV}^2$ in fig. 11). There is, however, a larger discrepancy for the case of the second sum rule.

This last point needs some discussion. The integrals $J_i(s_0)$, being over a finite range, are not quite equivalent to the Laplace transform sum rules given in eqs. (9) and (10). For the 1st Weinberg sum rule, assuming that the longitudinal structure functions are well approximated by their values in the chiral limit:

$$\rho_V^{(0)}(M^2) - \rho_A^{(0)}(M^2) \simeq -f_\pi^2 \delta(M^2) \quad (21)$$

one has

$$\begin{aligned} \int_0^\infty ds e^{-s/\kappa^2} (v(s) - a(s)) &= J_1(s_0) + \int_{s_0}^\infty ds e^{-s/\kappa^2} (v(s) - a(s)) \\ &= 4\pi \{ f_\pi^2 + \text{r.h.s. (eq. (9))} \}. \end{aligned} \quad (22a)$$

Similarly, for the second sum rule one deduces that

$$\begin{aligned} \int_0^\infty ds e^{-s/\kappa^2} s (v(s) - a(s)) &= J_2(s_0) + \int_{s_0}^\infty ds e^{-s/\kappa^2} s (v(s) - a(s)) \\ &= 4\pi \text{ r.h.s. (eq. (10))}. \end{aligned} \quad (22b)$$

For $\kappa^2 = 1.5 \text{ GeV}^2$, the numerical value of the κ^2 dependent terms on the r.h.s. of eqs. (9) and (10) are rather negligible compared to the values of $J_i(s_0)$ in figs. 11

and 12

$$4\pi \text{ r.h.s (eq. (9))} \approx 2 \times 10^{-4} \text{ GeV}^2, \quad (23a)$$

$$4\pi \text{ r.h.s. (eq. (10))} \approx 4\pi f_\pi^2 m_\pi^2 \approx 2 \times 10^{-3} \text{ GeV}^4. \quad (23b)$$

Therefore, if the tail integrals beyond s_0 were negligible, one would expect

$$J_1(s_0) \approx 4\pi f_\pi^2, \quad (24a)$$

$$J_2(s_0) \approx 0. \quad (24b)$$

As remarked above only (24a) seems to hold reasonably well. However, one can understand the reason for this discrepancy at least qualitatively.

We note first that there is an unavoidable uncertainty in our results due to the error inherent in extracting the spectral functions from the τ -decay data, which have both statistical and systematic errors. We estimate, however, that these errors can cause an uncertainty, for $s_0 = 2 \text{ GeV}^2$, of at most $\pm 0.01 \text{ GeV}^2$ and $\pm 0.01 \text{ GeV}^4$, for J_1 and J_2 , respectively. Hence, within our accuracy, $J_1(s_0)$ certainly agrees with the asymptotic value given in eq. (24a) but $J_2(s_0)$ does not. However, the tail integral for the second sum rule is *not* negligible, while it is much smaller for the first sum rule. To get an order of magnitude estimate of this effect – in the absence of data – we note from fig. 7 that, at $s = 2.5 \text{ GeV}^2$, $v(s) - a(s) \approx 0.05$. Clearly this difference will decrease as s increases and, as we will comment upon below, it should better change sign if one is to recover the expected results from QCD. Nevertheless, in magnitude, it seems reasonable to expect

$$|T_1| \leq 0.05 \int_{s_0}^{\infty} e^{-s/\kappa^2} ds = 0.05 \kappa^2 e^{-s_0/\kappa^2} \approx 0.014 \text{ GeV}^2, \quad (25a)$$

$$|T_2| \leq 0.05 \int_{s_0}^{\infty} e^{-s/\kappa^2} s ds = 0.05 \kappa^4 \left(1 + \frac{s_0}{\kappa^2}\right) e^{-s_0/\kappa^2} \approx 0.057 \text{ GeV}^4, \quad (25b)$$

where the numerical results in eq. (25) are those appropriate for the case $\kappa^2 = 1.5 \text{ GeV}^2$ and $s_0 = 2.5 \text{ GeV}^2$. We see from these equations that while the uncertainty of the tail integral for the first sum rule is of the order of the experimental uncertainty, for the second sum rule the tail integral is much more important. However, note that to recover the expected QCD prediction it is necessary that eventually, for some region of s , $a(s) > v(s)$, since the tail integrals *add* to J . The absence of any clear signal for the $\tau \rightarrow \nu_\tau 5\pi$ modes [14, 15] is in this sense rather perturbing. However, since asymptotically $a(s) = v(s) = 1/2\pi$, it is clear from fig. 7 that large variations in both $v(s)$ and $a(s)$ are still to be expected.

There is perhaps a bit more reliable way to gauge the effect of our lack of knowledge of the spectral functions beyond $s_0 \approx 2.5 \text{ GeV}^2$. This is to consider

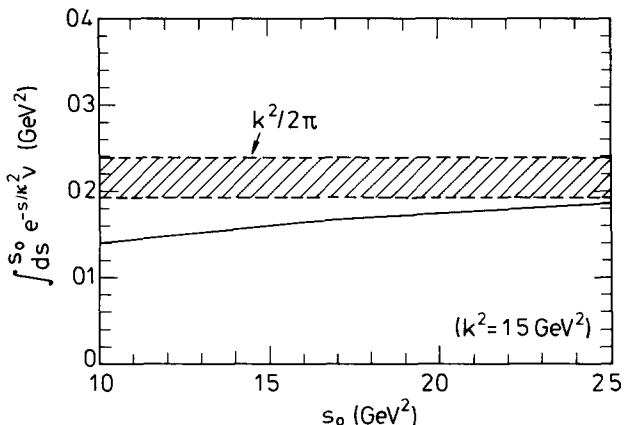


Fig. 13. Laplace transform behaviour of the vector spectral function. The shaded area defines the uncertainty between the strict asymptotic prediction, (upper straight line) and the prediction using our tail approximation (lower straight line)

directly the Laplace transform integrals of the vector and axial spectral functions *separately*. In this case, since the spectral functions are positive, the tail integrals are well under control. For the vector case, for instance, in the chiral limit, one has

$$\int_0^\infty dM^2 e^{-M^2/\kappa^2} v(M^2) = \frac{\kappa^2}{2\pi} + O(1/\kappa^4), \quad (26a)$$

$$\int_0^\infty dM^2 M^2 e^{-M^2/\kappa^2} v(M^2) = \frac{\kappa^4}{2\pi} + O(1/\kappa^2). \quad (26b)$$

We show in figs. 13 and 14 the above integrals with the integration being performed over a finite range, up to $s_0 = 2.5 \text{ GeV}^2$, for the case $\kappa^2 = 1.5 \text{ GeV}^2$. It is clear that the zeroth moment of the vector Laplace transform approaches much nearer to its asymptotic value than the first moment. The crosshatched area in the figures is just our estimate of the tail integral in which, for $v(s)$ above $s > 2.5 \text{ GeV}^2$, we have just used its asymptotic value: $v = 1/2\pi$. Thus

$$T_1^V = \frac{1}{2\pi} \int_{s_0}^\infty dM^2 e^{-M^2/\kappa^2} = \frac{\kappa^2}{2\pi} e^{-s_0/\kappa^2}, \quad (27a)$$

$$T_2^V = \frac{1}{2\pi} \int_{s_0}^\infty dM^2 M^2 e^{-M^2/\kappa^2} = \frac{\kappa^2}{2\pi} (s_0^2 + \kappa^4) e^{-s_0/\kappa^2}. \quad (27b)$$

As can be seen from the figures, these estimates for the tails are quite reliable. So

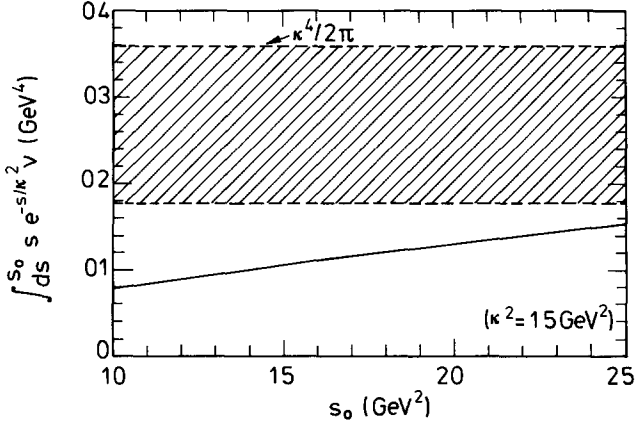


Fig. 14. As in fig 13 but now for the Laplace transform of the first moment of the vector spectral function. Here the uncertainty region is much bigger than in fig 13.

really, the principal problem in the second Weinberg sum rule is that the lack of positivity of $v(s) - a(s)$ does not allow for an accurate estimate of the tail remainder.

On balance, it appears that the spectral functions obtained from an analysis of the τ semileptonic decays display all of the qualitative features awaited in QCD. However, the narrow kinematical range available makes a direct quantitative comparison with detailed QCD predictions rather difficult. This is particularly so for the Weinberg sum rules since we are dealing with differences between spectral functions. For the Laplace transform version of the 1st Weinberg sum rule, within the uncertainties of the analysis, things seem to work rather well. The situation with the second Laplace transform sum rule is less clear, although qualitatively one has at least an understanding of why the discrepancy might be bigger here. Similar comments apply for $\pi^+ - \pi^0$ difference. Although a quantitative prediction is not possible, one understands qualitatively why a low-energy saturation of the formula of Das et al. [10] might well work, since there are piecewise cancellations between $v(s)$ and $a(s)$. In this respect, it would have been much nicer if the τ -lepton had had a mass of 5 GeV!

We would like to thank the Argus collaboration and in particular A. Golutvin and U. Binder for making their τ -lepton distributions available to us. We are grateful, furthermore, to B. Guberina for some very helpful discussions. One of us (J.S.) is deeply indebted to M. Martinez for his valuable help and advice in computational matters and would additionally like to thank M. Marquina, C. Mañá and L. Garrido for their assistance.

References

- [1] R.P. Feynman and M. Gell-Mann, *Phys. Rev.* 109 (1958) 193;
R.E. Marshak and E.C.G. Sudarshan, *Phys. Rev.* 109 (1958) 1860;
S.S. Gershtein and Y. Zeldovich, *Sov. Phys. JETP* 2 (1957) 576
- [2] M. Gell-Mann, *Phys. Rev.* 111 (1958) 362
- [3] J. Schwinger, *Phys. Rev. Lett.* 3 (1959) 235
- [4] S. Weinberg, *Phys. Rev. Lett.* 18 (1967) 507
- [5] E. Floratos, S. Narison and E. de Rafael, *Nucl. Phys.* B155 (1979) 115
- [6] M.A. Shifman, A.I. Vainshtein and V.I. Zakharov, *Nucl. Phys.* B147 (1979) 385
- [7] P. Pascual and E. de Rafael, *Z. Phys.* C12 (1982) 127
- [8] S. Narison, *Z. Phys.* C14 (1982) 263
- [9] R. Dashen, *Phys. Rev.* 183 (1969) 1245;
M. Gell-Mann, R. Oakes and B. Renner, *Phys. Rev.* 175 (1968) 2195
- [10] T. Das, G. Guralnik, V. Mathur, F. Low and J. Young, *Phys. Rev. Lett.* 19 (1967) 759
- [11] J. Gasser and H. Leutwyler, *Phys. Reports* 87C (1982) 77
- [12] K. Kawarabayashi and M. Suzuki, *Phys. Rev. Lett.* 16 (1966) 225;
K. Riazuddin and M. Fayazuddin, *Phys. Rev.* 147 (1966) 1071
- [13] Y.S. Tsai, *Phys. Rev.* D4 (1971) 2821
- [14] F.J. Gilman and S.H. Rhie, *Phys. Rev.* 31D (1985) 1066
- [15] B.C. Barish, Caltech preprint CALT-68-1321
- [16] A. Golutvin and U. Binder, private communication
- [17] H. Albrecht et al., preprint DESY-86-060
- [18] J.M. Yelton et al., *Phys. Rev. Lett.* 56 (1986) 812
- [19] D. Benaksas et al., *Phys. Lett.* 39B (1972) 289
- [20] W. Ruckstuhl et al., *Phys. Rev. Lett.* 56 (1986) 2132